ELSEVIER

Journal of Chromatography A, 806 (1998) 251–263

JOURNAL OF CHROMATOGRAPHY A

Sintered octadecylsilica as monolithic column packing in capillary electrochromatography and micro high-performance liquid chromatography

Reza Asiaie, Xian Huang, Dell Farnan, Csaba Horváth*

Department of Chemical Engineering, Yale University, New Haven, CT 06520-8286, USA

Received 30 October 1997; received in revised form 14 January 1998; accepted 16 January 1998

Abstract

Fused-silica capillaries were packed with porous 6-μm octadecylated silica microspheres and subjected to thermal treatment in order to obtain a column with porous silica based monolithic packing. After sintering, the monolithic packing was reoctadecylated in situ with dimethyloctadecylchlorosilane. The mechanical strength and stability of the monolithic column were significantly greater than those of conventional columns packed with particulate stationary phase. The performance of the columns was evaluated in both μ-HPLC and capillary electrochromatography (CEC) of small aromatic compounds and polycyclic aromatic hydrocarbons with 10 m*M* borate, pH 8.0, in acetonitrile–water mixtures as the mobile phase. Since no untoward bubble formation was observed, CEC could be performed in a CZE unit without the need for pressurizing the monolithic column. The plate efficiency of the monolithic column was similar to that of columns freshly packed with the same particles and was always higher in the CEC than in the μ-HPLC under otherwise identical conditions. The electrosmotic flow (EOF) velocity increased with the acetonitrile content of the eluent in open fused-silica capillaries with octadecylated innerwall and in columns packed with sintered octadecylsilica. In contradistinction, the EOF velocity decreased with the organic strength of the eluent in raw fused-silica capillaries. The opposite trend is attributed to the different effect of changing organic modifier concentration on the accessibility of silanol groups at the raw and octadecylated silica surfaces. © 1998 Elsevier Science B.V.

Keywords: Stationary phases, LC; Sintered octadecylsilica; Electrochromatography

1. Introduction

For capillary electrochromatography (CEC) to unfold its potential as a high-performance separation technique [1–4], further progress is required in the area of capillary column technology. Most columns employed in CEC and μ-HPLC are prepared by packing fused-silica capillaries of 20–100 μm I.D. with porous functionalized silica particles of 2–10 μm diameter. Performance and stability of such particulate packing greatly depend on the integrity of the retaining frits at the two ends of the column to keep the packing in place and hinder the movement of charged particles in high electric field. Formation of discontinuities in the bed structure due to dislocation of particles is referred to as gapping. It occurs frequently in practice and diminishes the separation efficiency of conventionally packed columns. These

*Corresponding author.

0021-9673/98/$19.00 © 1998 Elsevier Science B.V. All rights reserved.
PII S0021-9673(98)00052-1

problems have prompted our present investigation of the potential of monolithic porous packings that require no frits to stay in place and are expected to be stable without gapping over an extended period of operational time.

The first polymeric column packings prepared in situ for gas and liquid chromatography were based on polyurethane [5,6]. More recent developments include, in situ preparation of a compressed ''continuous bed'' of polyacrylamide gel [7,8] for conventional and μ-HPLC and a ''molded continuous rod'' of methacrylic polymer [9] for conventional HPLC. Reversed-phase columns prepared with a monolithic gel matrix of acrylamide and methacrylate monomers with octadecyl functions have been used in CEC of polycyclic aromatic hydrocarbons [10] and efficiencies as high as 120 000 theoretical plates/m were obtained with a 25 μm inner diameter column. Very recently, ''molded'' rigid monolithic columns prepared by copolymerization of ethylene dimethacrylate, butyl methacrylate, and 2-acrylamido-2-methyl-1-propanesulfonic acids have been used in reversed-phase CEC [11]. Octadecylated porous silica monolith was prepared in situ by acid-catalyzed hydrolysis/condensation of tetramethoxysilane for conventional HPLC [12] and from potassium silicate and dimethyloctadecylchlorosilane for μ-HPLC [13]. In situ polymerization promises to yield higher porosities and permeabilities of the columns than those obtained with conventional packed columns. Furthermore, enhanced column stability can also be expected as a result of the in situ formed monolithic packing.

In another approach, a conventionally packed capillary column is converted into one with a monolithic packing by irreversibly agglomerating the stationary phase particles to form a monolithic structure. The column thus obtained has a porosity similar to that of the starting column and the rationale for the treatment is to impart mechanical stability to the packing. However, a significant advantage of the latter method is the possibility of using well characterized stationary phase particles, e.g., silica based bonded phases of desired particle size, pore dimensions and functionalization. Indeed, it has been shown recently [14] that, by cementing siliceous particles such as those employed in reversed-phase chromatography, monolithic columns can be obtained that are very stable under the operating conditions in CEC.

Although the works cited above are quite promising, further research is required to obtain novel types of packed capillaries with greatly improved column stability, versatility and reproducibility. In the present work, the preparation of monolithic columns by sintering of octadecylsilica particles packed in fused-silica capillaries is discussed and their properties in reversed-phase CEC are characterized.

2. Experimental

2.1. Chemicals and materials

Reagent grade sodium dihydrogenphosphate monohydrate, disodium hydrogenphosphate, boric acid and sodium bicarbonate were purchased from J.T. Baker (Phillisburg, NJ, USA). Thiourea and HPLC-grade acetonitrile, acetone and toluene were obtained from Fisher Scientific (Pittsburgh, PA, USA). Sodium hydroxide and pyridine were purchased from Mallinkrodt (Paris, KY, USA) and formamide and dimethyloctadecylchlorosilane were provided by Eastman Kodak (Rochester, NY, USA) and Hüls Petrarch Systems (Bristol, PA, USA), respectively. The polycyclic aromatic hydrocarbon samples, naphthalene, biphenyl, fluorene, phenanthrene, fluoranthene, *m*-terphenyl and benzaldehyde were purchased from ChemServices (West Chester, PA, USA). Benzyl alcohol and the PTH amino acid derivatives of asparagine (N), glutamine (Q), threonine (T), Glycine (G), alanine (A), and tyrosine (Y) were obtained from Sigma (St. Louis, MO, USA).

The sodium phosphate and sodium borate buffers were prepared by diluting a 50 or a 100 m*M* stock solution to the desired concentrations with appropriate volumes of water and acetonitrile. In this manner, the salt concentration is kept constant in all hydro–organic mobile phases used in this study. The buffers were filtered through a 0.45 μm pore size MicronSep nitrocellulose filter (Micron Separation, Westborough, MA, USA). The water was purified and deionized with a Nanopure system (Barnstead, Boston, MA, USA).

Fused-silica capillaries with polyimide outer coat-

ing of either 50 or 75 μm I.D. and 375 μm O.D. were purchased from Quadrex (New Haven, CT, USA). Silica particles with 2-μm diameter were from Glycotech (Hamden, CT, USA) and Zorbax octadecylsilica particles with 6-μm diameter and 80 Å mean pore diameter were complementary samples from Rockland Technologies (Newport, DE, USA).

2.2. Apparatus

A detailed description of the electrochromatograph is described by Choudhary et al. [15]. It featured a 90 kV dual power supply (Spellman, Plainview, NY, USA) and a Spectra FOCUS (Thermo Separation Products, Fremont, CA, USA) detector for on-column detection. The inlet and outlet vials are housed in two chambers, which can be pressurized with an inert gas up to 10 bar. However, in the present work the column inlet and outlet were maintained at atmospheric pressure without untoward bubble formation. The minimum lengths from the column inlet to the detector window and from the window to the column outlet were 20 and 10 cm, respectively. An OS/2 supported PC 1000, version 3.0 (Thermo Separation Products) and a Model PS/2 77 486 computer (IBM, FL, USA) were used to control the experimental conditions and to acquire data.

Electrophoretic experiments with the raw capillaries and those having octadecylated innerwall were performed with a Beckman (Fullerton, CA, USA), Model P/ACE 2200 CZE unit equipped with a UV-detection system. Beckman System Gold software and a PowerMate SX/20 computer (NEC Technologies, Boxborough, MA, USA) were used for instrumental control and data acquisition.

All μ-HPLC experiments were performed by using a modified Hewlett-Packard Model 1090 (Palo Alto, CA, USA) liquid chromatograph equipped with a DRV 5 high-performance pumping system and an autoinjector. The flow from the 1090 was split after the injection valve using a TEE-piece from Upchurch Scientific (Oak Harbor, WA, USA) and the column was attached at a right angle to the fluid inlet of the TEE with the restriction capillary directly opposite the fluid inlet. This orientation of the TEE reduced the fouling of the column and brought about higher separation efficiency in terms of increased plate numbers. The split ratio was adjusted by the length and diameter of the capillary restrictor attached to the TEE and was about 4000:1. A Thermo Separations UV 2000 (Fremont, CA, USA) dual wavelength UV–Vis detector fitted with a capillary flow cell was placed at the same level as the injection valve in close proximity to the left hand side of the chromatograph to minimize the length of the connecting tubing. Data was collected using a DOS version 1.1 of the Hewlett-Packard Chemstation software, which was installed on a Hewlett-Packard Vectra 486DX33 IBM compatible computer running windows 3.1 operating system. Connection of the UV 2000 detector to the computer was achieved through a Hewlett-Packard Model 35900 analog/digital interface.

The Model ISI SS-40 scanning electron micrograph (International Scientific Instruments, Santa Clara, CA, USA) was operated at 10 kV and at a filament current of 40 mA. The samples were first mounted by placing an approximately 2 mm long piece of the capillary on an aluminum stub via a double sided carbon tape (Electron Microscopy Sciences, Ft. Washington, PA, USA). Then they were sputter coated with gold/palladium alloy by a SPI Sputter (SPI Supplies Division of Structure Probe, West Chester, PA, USA) for 25 s at 30 mA to prevent charging.

2.3. Procedures

2.3.1. Preparation of the packed capillaries

The column packing technology was similar to that described in the literature [14–18]. One end of the fused-silica capillary (75 μm×40 cm) was tapped in 2-μm fused-silica microspheres (Glycotech, Hamden, CT, USA) until a 200–300 μm long packing was obtained. A Type 3A Blowpipe (Veriflo, Richmond, VA, USA) with oxygen/butane fuel was used to heat the column end to make a retaining frit by sintering the particles. Stability of the frit was tested at pressures up to 400 bar by pumping water with a Model ConstaMetric III pump (Milton Roy, LDC Division, Riviera Beach, FL, USA). The capillary was first connected to a stainless steel reservoir (50 mm long×2 mm I.D.) then it was filled with a 2% (w/v) slurry of the siliceous particles in a 1:1 mixture of toluene and acetone. Thereafter, acetone, the packing solvent, was

pumped by an Altex Model 100A metering pump (Beckman) at 500 bar for 2 h. Then after removing the reservoir and connecting the capillary directly to the pump, the pressure was increased to 600 bar and the acetone flow was maintained for 10 h.

The packed column was washed with water at 150 bar for 60 min to remove acetone. Subsequently, while maintaining the 150 bar inlet pressure by pumping water through the column, at a distance of about 15 cm from the pump, a narrow segment of the column was heated electrically with a Ni/Cr wire loop in order to prepare the outlet retaining frit. The pressure was then released, the column was removed from the pump, and the retaining frit which was originally made to hold the packing in place was cut off. Then the column was connected to the pump from this end and washed again with water at 150 bar to remove the excess siliceous packing from the capillary downstream of the outlet frit. The detection window of about 2 mm in length was made by burning off the polyimide coating at the outlet frit. Finally, while still washing with water under pressure the inlet frit was prepared by the method described above, at a distance of about 1 cm from the pump.

2.3.2. Sintering procedure

The sintering of the packed capillaries was a three step process. First, the packed capillaries were rinsed with 0.1 *M* $NaHCO_3$ for 5 min, then with water and finally with acetone. The column was also purged with N_2 gas for at least 1 h for rapid drying. The second step was heating in a Model DP-41 vacuum oven (American Scientific Products, New York, NY, USA) at 120°C for 5 h. In the final step the column was heated with a Model 8500 capillary GC oven (Perkin Elmer, Norwalk, CT, USA) at 360°C for 10 h. The sintered columns were then washed with acetone to remove residues formed in the heat treatment.

2.3.3. Octadecylation procedure

In situ octadecylation was performed by pumping a solution of 20% (v/v) dimethyloctadecylchlorosilane and 10% (v/v) pyridine in toluene through a reservoir (32 mm long, 4 mm I.D.) and then through the packed capillary which was heated in a Model SSI 505 LC column oven (Scientific Systems, State College, PA, USA) at 100°C for 6 h. The duration of this procedure also allowed for the subsequent washing of the octadecylated packed column with acetone, which was used as the packing solvent. The same solution was also used for the in situ octadecylation of the open fused-silica capillaries. The capillary was first filled with the dimethyloctadecylchlorosilane solution, both ends were sealed, and then heated at 95°C for 5 h. After washing the capillary with acetone, the process was repeated.

3. Results and discussion

3.1. Column preparation

The packings of capillary columns obtained by sintering at 260 and 360°C without and at 360°C with sodium bicarbonate treatment are shown by the scanning electron micrographs in Fig. 1. Though raising the sintering temperature from 260 to 360°C was sufficient to immobilize the silica particles (Fig. 1A,B), stable packing was only obtained when there was partial fusion with grain boundary formation between the particles (Fig. 1C). It is noted that the treatment with sodium bicarbonate, which served as a flux, was necessary to obtain a stable monolithic packing. The effect of sintering is schematically illustrated in Fig. 2, where the sintered packing is distinguished by neck growth between silica particles and by partial adhesion of the particles to the fused-silica wall.

Sintering of amorphous or crystalline particles, is the conversion of a compacted powder into a monolith in which particles are joined to one another by grain boundaries [19]. In the process with increasing temperature, particles contact first, followed by alteration of the surface morphology by interparticle neck formation and fusion, and ultimately upon high temperature heating pore closure occurs [20]. For this reason, our concern was to find a sintering temperature at which the silica gel particles enter in neck formation, but no pore or channel closure occurs.

This is a result of a flux created during heating by the presence of a lower melting vitreous phase rich in sodium silicate formed in the presence of

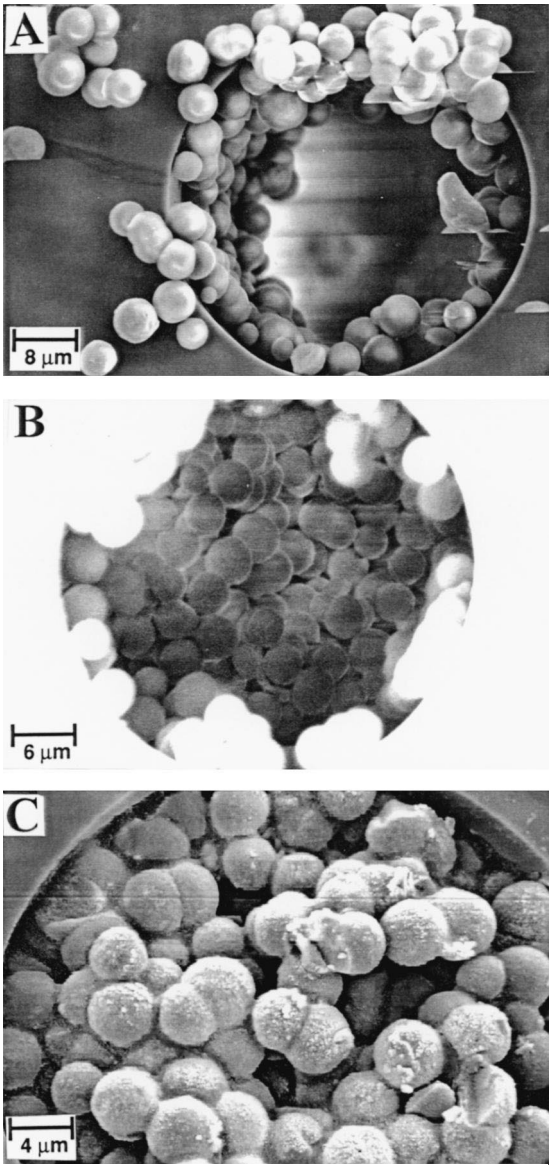

Fig. 1. Scanning electron micrographs of the packed fused-silica capillaries sintered at (A) 260°C and (B) 360°C without, and (C) at 360°C with $NaHCO_3$ flux.

$NaHCO_3$ which wets and partially dissolves the surface of the solid [20,21]. The surface tension forces will then pull the mass of the particles together, thereby forming interparticle boundaries. It should be noted that at the sintering temperature of 360°C the pore structure of silica will remain essentially unchanged since crystallization and complete

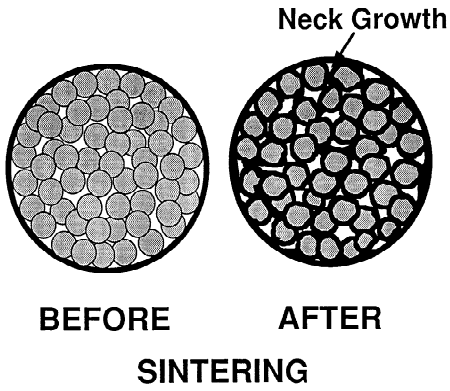

Fig. 2. Schematic illustration of the effect of sintering on the octadecylated silica packing in fused-silica capillaries.

pore closure of silica occurs at temperatures above 1000°C [19]. The consequence of neck sintering of the silica gel particles is to impart stability to the chromatographic column bed and to maintain the porous structure of the packing material.

The effect of temperature on the structure of amorphous silica has extensively been studied [22–24]. Irreversible destruction of the pore structures in silica has been observed only at temperatures above 600°C. However, in the sintering conditions of this study, the silica particles go through reversible dehydration and dehydroxylation processes. The former occurs in the first step of sintering at 120°C, in which the physically adsorbed water is removed. The dehydroxylation of the vicinal silanol groups occurs at higher temperatures (200 to 500°C). This follows the stabilization of crystalline silica, quartz at 600°C, with a complete condensation of both the vicinal and the isolated silanol groups.

The results in this study, were obtained with capillaries packed with octadecylated silica particles, and after sintering the octadecylated surface was rejuvenated. Some experiments were conducted with capillary columns packed with raw silica, by using the same method, and subsequently octadecylated. Whereas the retentive properties of all columns were about the same, the packing of the raw silica was a much less reproducible process and the column thus obtained showed significantly lower reproducibility and stability than the column packed with octadecylated silica. The improvements upon sintering octadecylsilica rather than raw silica have been

unexpected. One of the possible explanations attributes the effect to the greater water binding to the raw silica than to the octadecylated silica even after the drying step at 120°C. As a result, less water is liberated during the subsequent sintering step in columns packed with octadecylated particles so that bed rupture and concomitant gapping due to sudden bursts of water vapor can be avoided.

3.2. Effect of acetonitrile concentration on EOF velocity

It is widely believed that the generation of EOF in both packed and open capillaries is governed by the same principle [25,26]. The EOF velocity, u_{eo}, at a charged surface in an electric field, E, was expressed by von Smoluchowski [27] as:

$$u_{eo} = \varepsilon_0 \varepsilon_r \zeta E/\eta, \quad (1)$$

where, ε_0, ε_r, η and ζ are the permittivity of vacuum, the dielectric constant of the eluent, the viscosity of the solvent, and the zeta potential, respectively. The mobility of an inert uncharged tracer, μ_{eo}, is taken as the measure of EOF [15]. It is evaluated from the migration distance, L, electric field strength and the migration time, t_{eo}, of the inert uncharged tracer by:

$$\mu_{eo} = L/t_{eo}E = u_{eo}/E. \quad (2)$$

As suggested by Eq. (1) and shown experimentally, the composition of the hydro–organic mobile phase affects the magnitude of EOF [4,28]. We have measured the effect of the organic modifier concentration on the EOF velocity obtained with a monolithic octadecylated silica column and with two open fused-silica capillaries, one raw and one having an octadecylated innerwall. Plots of the EOF velocity and the current versus the electric field strength with the acetonitrile concentration as the parameter are shown in Fig. 3. It is seen that the EOF velocity increases linearly with the field strength and decreases with the acetonitrile concentration in the experimental range. Plots of the EOF velocity as a function of the acetonitrile concentration with the field strength as the parameter have a shallow minimum at approximately 40% (v/v) acetonitrile as seen in Fig. 4.

The dependence of EOF velocity on the nature and

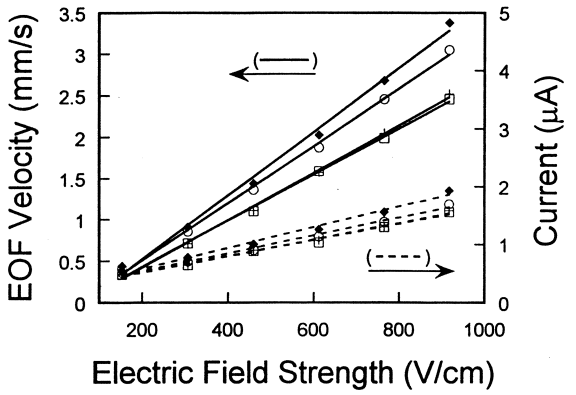

Fig. 3. Plots of current (dashed lines) and electrosmotic velocity (solid lines) as a function of the overall electric field strength with the acetonitrile concentration in the mobile phase as the parameter: (+) 20, (□) 40, (○) 60, (♦) 80% (v/v). Column, 75 μm×23/33 cm, monolithic packing of sintered and reoctadecylated 6-μm Zorbax-ODS (80 Å); mobile phase, acetonitrile–water mixtures containing 10 m*M* sodium borate, pH 8.0; detection, 214 nm; electrokinetic injection, 1 s, 5 kV; EOF marker, 2 μl/ml formamide in the mobile phase.

concentration of the organic modifier in raw fused-silica capillaries packed with octadecylated silica has been controversial [4,29–33]. In certain cases, the contradictory behavior was due to differences in the

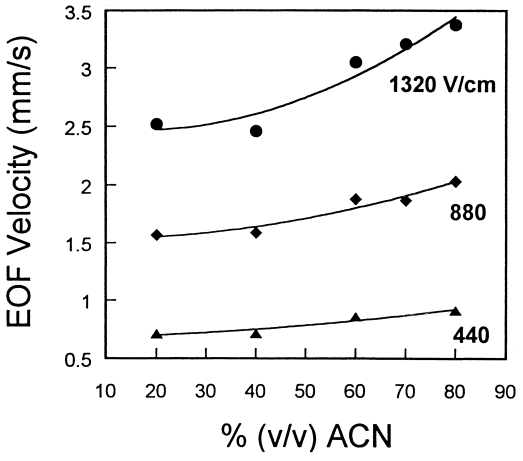

Fig. 4. Plots of the electrosmotic velocity as a function of the acetonitrile concentration with the field strength as the parameter. Column, 75 μm×23/33 cm, monolithic packing of sintered and reoctadecylated 6-μm Zorbax-ODS (80 Å); mobile phase, acetonitrile–water mixtures containing 10 m*M* sodium borate, pH 8.0; detection, 214 nm; electrokinetic injection, 1 s, 5 kV; EOF marker, 2 μl/ml formamide in the mobile phase.

preparation of the hydro–organic buffers serving as the mobile phase. Other observations support the notion that the increase in the EOF velocity with the acetonitrile concentration is to be attributed to acetonitrile mediated changes at the octadecylated surface of the siliceous stationary phase [18,31].

Fig. 5 illustrates the quasilinear adsorption isotherm of acetonitrile on tetradecylated silica from aqueous solution [34,35]. Fig. 5 also shows a plot of the ratio of dielectric constant to the viscosity, ε/η, against acetonitrile concentration in aqueous solution [28,36]. The curve representing the ε/η ratio reaches a minimum at about 40% acetonitrile, and in view of Eq. (1), this finding is consistent with the results that the EOF velocity increases with increasing acetonitrile concentration as shown in Fig. 4. Nonetheless, the data presented in Figs. 4 and 5 are insufficient to support the observed dependence of EOF velocity on the acetonitrile concentration.

Further insight is gained by comparing the effect of acetonitrile concentration on EOF in raw and octadecylated fused-silica capillaries. In open raw capillaries the mobility of the inert tracer decreases with increasing organic modifier concentration as seen in Fig. 6. However, in the octadecylated open capillary it increases with the organic strength of the mobile phase under otherwise same conditions. This behavior is also exhibited by the capillary packed with octadecylated monolithic support, as shown in Fig. 6. The data presented here are average electrosmotic mobilities measured at five different voltages at each acetonitrile concentration. The electric field strength across the packed segment of the duplex CEC column and the electrosmotic mobilities were calculated by using Ohm's law [15]. Since current is preserved throughout the duplex column, conductances of the packed and open segments are different.

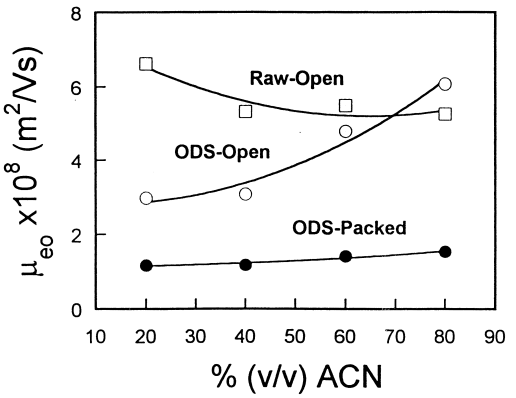

Fig. 6. Plots of electrosmotic mobility as a function of acetonitrile concentration. (●) 75 μm×23/33 cm fused-silica capillary with monolithic packing of sintered and reoctadecylated 6-μm Zorbax-ODS (80 Å), (○) 50 μm×20/27 cm open fused-silica capillary with octadecylated innerwall and (□) 50 μm×20/27 cm raw open fused-silica capillary. Mobile phase: acetonitrile–water mixtures containing 10 m*M* sodium borate, pH 8.0; detection, 214 nm; electrokinetic injection, 1 s, 5 kV; EOF marker, 2 μl/ml formamide in the mobile phase.

The EOF velocities in the octadecylated open capillaries with 10 m*M* sodium borate, pH 8.0, and a 20/27 cm long column, ranged from 1.1–2.4 mm/s at 10 kV and 3.4–6.1 mm/s at 30 kV at 20 and 80% acetonitrile concentrations, respectively. Comparable values for the 23/33 cm long octadecylated packed capillaries were in the range of 0.7–0.9 mm/s at 10 kV and 2.5–3.4 mm/s at 30 kV. The data shown in Fig. 5 strongly indicate that the properties of the bulk mobile phase alone do not account for the effect of organic modifier on EOF. If variations in EOF depended only on the changes in the ε/η ratio, the magnitude of EOF would increase with the organic strength in both capillaries having either a raw or octadecylated surface [27].

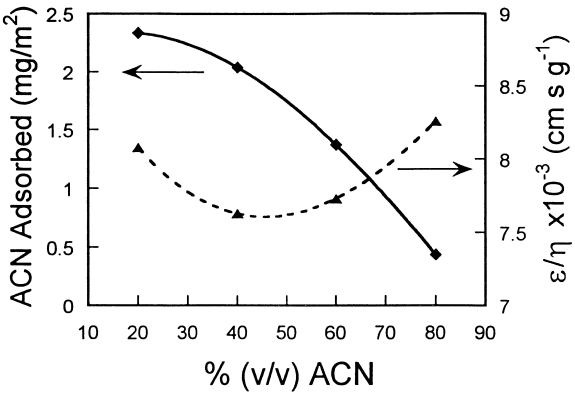

Fig. 5. The adsorption isotherm of acetonitrile on tetradecylated silica from aqueous solution at 20°C is adapted from Ref. [35] and shown by solid lines. Plots of the ε/η ratio versus the composition of acetonitrile–water mixtures are adapted from Refs. [28,36] and shown by dashed lines.

3.3. CEC separation of PAHs and PTH-amino acids

The separation of six polycyclic aromatic hydrocarbons (PAHs) is shown by the two electrochromatograms depicted in Fig. 7. The mobile phase in either 60 or 80% (v/v) aqueous acetonitrile was 10 m*M* sodium borate, pH 8.0, and formamide was used as the uncharged inert tracer. The retention factors were measured with the sintered and in situ reoctadecylated column as a function of acetonitrile concentration. The results are presented in Fig. 8 by plots of the logarithmic retention factor, κ, versus the acetonitrile concentration, φ, given in percent (v/v). As customary in reversed-phase chromatography, the plots are linear with negative slopes. Retention factors for naphthalene and *m*-terphenyl were 1.3 and 4.0 at 80% acetonitrile and 5.3 and 26 at 60% acetonitrile, respectively. Similar κ values have been reported in the literature for the retention of biphenyl on an ODS-LiChrospher column in a 80:20 (v/v) % acetonitrile–borate buffer. On the other hand, the κ values were lower, in the range of -0.24 to 0.28 for naphthalene, fluorene and phenanthrene with the same mobile phase on a Hypersil-ODS column [18,31].

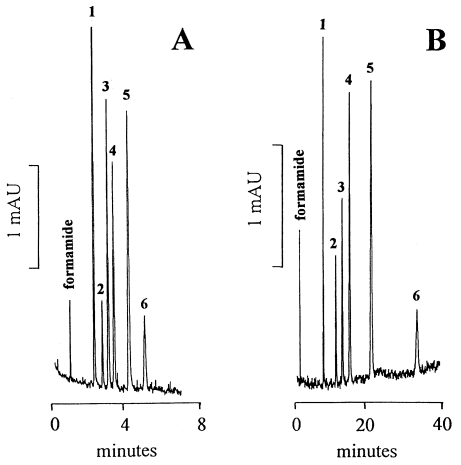

Fig. 7. Electrochromatograms of polycyclic aromatic hydrocarbons. (A) 80% (v/v) and (B) 60% (v/v) acetonitrile in the mobile phase. Column, 75 μm×23/33 cm, monolithic packing of sintered and reoctadecylated 6-μm Zorbax-ODS (80 Å); mobile phase, % (v/v) acetonitrile in 10 m*M* sodium borate, pH 8.0; applied voltage, 30 kV; detection, 214 nm; electrokinetic injection, 2 s, 5 kV; sample, 50–200 mg/ml dissolved in the mobile phase. Order of elution, formamide (1 μl/ml), naphthalene (1), biphenyl (2), fluorene (3), phenanthrene (4), fluoranthene (5) and *m*-terphenyl (6).

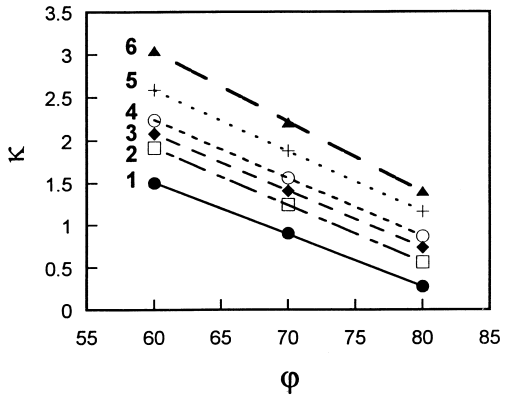

Fig. 8. Plots of κ versus φ for polycyclic aromatic hydrocarbons. Naphthalene (1), biphenyl (2), fluorene (3), phenanthrene (4), fluoranthene (5) and *m*-terphenyl (6). Column, 75 μm×23/33 cm, monolithic packing of sintered and reoctadecylated 6-μm Zorbax-ODS (80 Å); mobile phase, acetonitrile–water mixtures containing 10 m*M* sodium borate, pH 8.0; EOF marker, formamide; detection, 214 nm; electrokinetic injection, 2 s, 5 kV; sample, 50–200 mg/ml dissolved in the mobile phase.

The monolithic column was used for the separation of phenylthiohydantoin (PTH) derivatives of amino acids [37–39]. Generally, reversed-phase HPLC [40] is the technique of choice for their analysis, micellar electrokinetic capillary chromatography (MEKC) [41–43] have also been used. Recently, capillary electrochromatography (CEC) was also used with both isocratic and gradient elution to separate PTH-amino acids [16]. Fig. 9 illustrates the electrochromatogram of six PTH-amino acids obtained by using CEC with a monolithic and in situ octadecylated column. The order of elution follows the increase in their hydrophobic character as in reversed-phase HPLC. The separation is comparable to that in HPLC [37].

Bubble formation in reversed-phase CEC has often been reported and recommended to keep the two ends of the column under pressure to suppress the formation of bubbles during the chromatographic runs [1,17,32,33]. The electrochromatograms in Figs. 7 and 9 were obtained by keeping the inlet and outlet of the column at atmospheric pressure. The applied voltages were 15 and 20 kV, and the mobile phase was 5 m*M* sodium phosphate, pH 7.50, with 30%

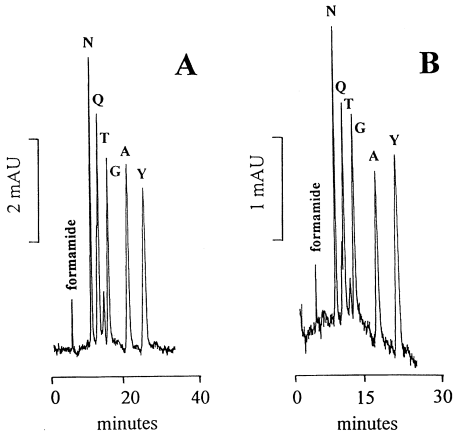

Fig. 9. Electrochromatograms of the PTH amino acids obtained at two different applied voltages. (A) 15 kV and (B) 20 kV, column: 75 μm×23/33 cm, monolithiic packing of sintered and reoctadecylated 6-μm Zorbax-ODS (80 Å); mobile phase, 30% (v/v) aqueous acetonitrile containing 5 m*M* sodium phosphate, pH 7.5; detection, 214 nm; electrokinetic injection, 2 s, 5 kV; sample, 15–30 μg/ml dissolved in the mobile phase. Order of elution, formamide (1 μl/ml), PTH-asparagine (N), PTH-glutamine (Q), PTH-threonine (T), PTH-glycine (G), PTH-alanine (A) and PTH-tyrosine (Y).

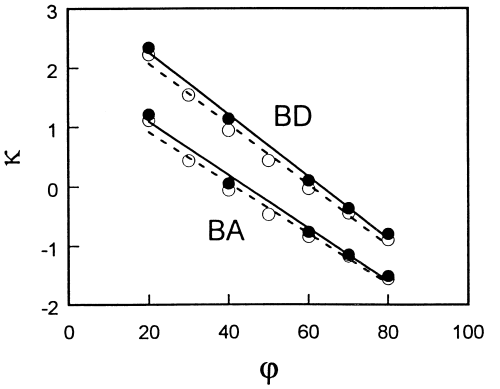

Fig. 10. Plots of the logarithmic retention factors obtained with the same column in reversed-phase CEC and μ-HPLC versus φ for benzyl alcohol (BA) and benzaldehyde (BD). Column, 75 μm× 23/33 cm, monolithic packing of sintered and reoctadecylated 6-μm Zorbax-ODS (80 Å); mobile phase, acetonitrile–water mixtures containing 10 m*M* sodium borate, pH 8.0; EOF marker, thiourea (0.2 mg/ml); detection, 214 nm; sample, 1–2 μl/ml dissolved in the mobile phase. (●) CEC; electrokinetic injection, 1 s, 5 kV, and (○) μ-HPLC; injection, 5 μl.

acetonitrile. The absence of bubbles in CEC analysis at atmospheric pressure with the monolithic column is believed to be due to the uniform structure of the sintered column packing that is readily wetted by hydro–organic eluents over a wide composition range. Indeed, the great advantage of the monolithic column is the absence of the retaining frits which are implicated in bubble formation for having surface properties different from those of the column packing. From this it may follow that octadecylation of the silica frits could reduce bubble formation in columns for reversed-phase CEC.

3.4. Comparison of μ-HPLC and CEC results with the same column

The monolithic column was used for the separation of small aromatic compounds in both CEC and μ-HPLC under otherwise identical conditions in order to assess the effect of the electric field on the separation, and to compare the efficiency and the retention characteristics of the same column in the two modes of chromatography. Fig. 10 shows κ versus φ plots obtained in these experiments with thiourea as the neutral tracer for measuring u_{eo}. As expected from the data shown in Fig. 8 above, the retention increased in a linear fashion with decreasing acetonitrile concentration. The retention factors of the two aromatic compounds shown in Fig. 10 were nearly the same in CEC and μ-HPLC. In comparison with the retention factors of the PAHs in Fig. 8, the slope of the lines were higher than with benzyl alcohol and benzaldehyde in Fig. 10, reflecting the higher contact area of the PAHs upon binding to the alkylated chromatographic surface. Fig. 11 shows the electrochromatograms of benzyl alcohol and benzaldehyde at 20 and 80% acetonitrile in sodium borate, pH 8.0. It is recalled that all CEC experiments were carried out without pressurization of the column.

Efficiency of the monolithic column in terms of the plate height was measured in both CEC and μ-HPLC by using the same mobile phase and formamide as the unretained tracer. The data were analyzed by using the simplified van Deemter equation [44]. It is given by:

$$H = A + B/u + Cu \quad (3)$$

where H is the plate height and u is the mobile phase

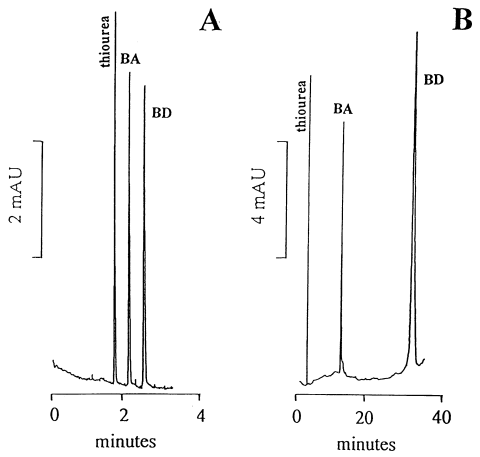

Fig. 11. Electrochromatograms of benzyl alcohol (BA) and benzaldehyde (BD) obtained in reversed-phase CEC at different acetonitrile concentrations in the mobile phase. (A) 80% (v/v) and (B) 20% (v/v) acetonitrile in the aqueous mobile phase. Column, 75 μm×23/33 cm, monolithic packing of sintered and reoctadecylated 6-μm Zorbax-ODS (80 Å); mobile phase, acetonitrile–water mixtures containing 10 m*M* sodium borate, pH 8.0; EOF marker, thiourea (0.2 mg/ml); applied voltage, 20 kV; detection, 214 nm; electrokinetic injection, 1 s, 5 kV; sample, 1–2 μl/ml dissolved in the mobile phase. Order of elution: thiourea, benzyl alcohol, benzaldehyde.

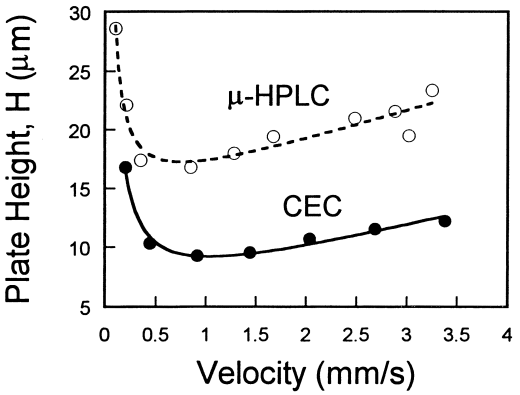

Fig. 12. Plots of the plate height versus the mobile phase velocity. The data was obtained with the same column in CEC (●); electrokinetic injection, 1 s, 5 kV, and in (○) μ-HPLC; injection, 5 μl. Column, 75 μm×23/33 cm, monolithic packing of sintered and reoctadecylated 6-μm Zorbax-ODS (80 Å); mobile phase, 80% (v/v) aqueous acetonitrile in 10 m*M* sodium borate, pH 8.0; detection, 214 nm; unretained neutral tracer, 2 μl/ml formamide in the mobile phase.

velocity, A is the so-called eddy diffusion term, B/u measures the contribution of longitudinal molecular diffusion to band spreading, and the C-term that of intraparticle mass transfer resistances. The results are illustrated in Fig. 12 by plots of the plate height versus the linear velocity and the efficiency parameters are listed in Table 1. Comparison of the A and the C terms of the van Deemter equation, each obtained by the two modes of chromatography, shows that the A and the C terms were larger by a factor of 2.7 and 1.5 in μ-HPLC than in CEC, respectively. The relatively high A ratio implies that band spreading due to nonuniformities of the packing structure is greater with viscous flow than with EOF in agreement with recent findings in our laboratory (unpublished results). The magnitude of the C ratio reflects an attenuation of the mass transfer resistance inside and/or at the surface of the stationary phase particles. The pore size of the silica support before octadecylation was 80 Å, i.e. narrow enough to preclude any substantial intraparticulate EOF which is found with wide pore supports (unpublished results). In agreement with the above observations, the minimum plate height was larger in μ-HPLC than in CEC by a factor of 2, whereas the optimum linear velocity was lower in μ-HPLC than CEC.

The influence of the acetonitrile concentration on the column efficiency, measured with formamide and on the retention of PAHs has been examined. The plate height is plotted against the migration velocity of formamide, which is widely used as a neutral and unretained tracer, at various acetonitrile concentrations which are illustrated in Fig. 13. In all cases, the values of H_{min} were between 8 to 10 μm at ''optimal'' EOF velocities of 0.7–0.9 mm/s. The curves become flatter with increasing acetonitrile concentration, suggesting higher intraparticle diffusion rates upon decreasing viscosity. Interestingly, at 40%

Table 1
Efficiency characteristics of the monolithic column prepared with 6-μm octadecylated silica particles and evaluated in μ-HPLC and CEC

Characteristics	μ-HPLC	CEC
H_{min} (μm)	16	8
V_{opt} (mm/s)	0.76	1.0
A (μm)	13.2±1.01	4.83±0.58
C (10^{-3} s)	3.14±0.38	2.12±0.21

Experimental conditions are described in Fig. 12.

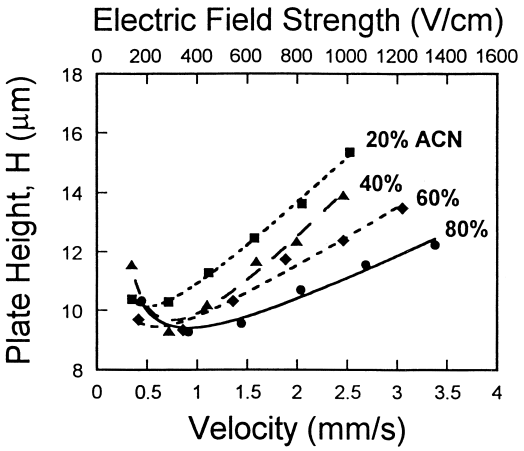

Fig. 13. Plots of the plate height measured with formamide as a function of the electrosmotic velocity with the acetonitrile concentration in the mobile phase as the parameter: (■) 20, (▲) 40, (♦) 60 (●) 80% (v/v). Column, 75 μm×23/33 cm, monolithic packing of sintered and reoctadecylated 6-μm Zorbax-ODS (80 Å); mobile phase, acetonitrile–water mixtures containing 10 m*M* sodium borate, pH 8.0; detection, 214 nm; electrokinetic injection, 1 s, 5 kV; EOF marker, 2 μl/ml formamide in the mobile phase.

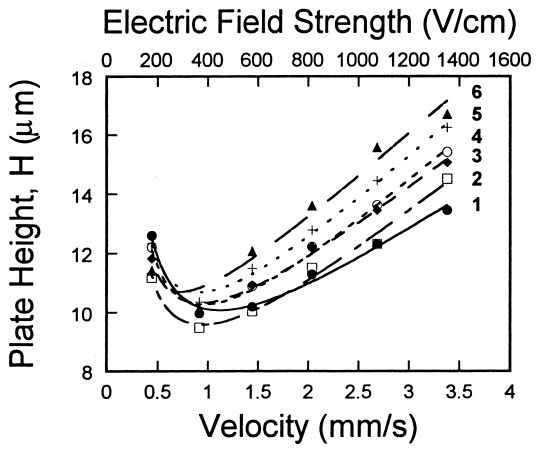

Fig. 14. Plots of plate height as measured with PAHs versus EOF velocity. Column, 75 μm×23/33 cm, monolithic packing of sintered and reoctadecylated 6-μm Zorbax-ODS (80 Å); mobile phase, 80% (v/v) aqueous acetonitrile containing 10 m*M* sodium borate, pH 8.0; detection, 214 nm; electrokinetic injection, 2 s, 5 kV; EOF marker, formamide (2 μl/ml); sample, 50–200 mg/ml dissolved in the mobile phase; 1, Naphthalene (1.3); 2, biphenyl (1.7); 3, fluorene (2.1); 4, phenanthrene (2.4); 5, fluoranthene (3.2); and 6, *m*-terphenyl (4.0). The numbers in the brackets are the retention factors (k') of the components.

acetonitrile, the ε/η ratio vide Eq. (1) is a minimum, and the slope (the *C*-term) of the van Deemter curve reaches a maximum. In Fig. 14, van Deemter plots of the PAHs are illustrated. The mobile phase was 10 m*M* sodium borate, pH 8.0, in 80% (v/v) aqueous acetonitrile and, as expected [45], the results show that the *C*-term increases with the retention factor. Plate numbers for the unretained peaks were in the range of 30 000–40 000 and those for the 6 PAHs were 25 000–35 000 using a 23/33 cm long column.

3.5. Reproducibility of measurements and column stability

Microscopic examination of short lengths (2–3 mm) of the monolithic column cut from the inlet end in weekly time intervals did not reveal any structural changes due to the intensive analytical use of the column. The migration velocities of formamide and the 6 PAHs were measured with different mobile phases in a randomized fashion in order to assess the stability of the monolithic column and the reproducibility of the measurements. For every experiment, the column was equilibrated with the mobile phase for 30 min or until the attainment of a stable baseline, prior to the EOF velocity measurements. The performance of the monolithic column remained essentially constant within the 30 day period of this series of experiments. The EOF velocities as measured with 20 and 80% acetonitrile in the mobile phase varied only by 2–3% within 30 days and after 300 chromatographic runs. The reproducibility of the results obtained with the 6 PAHs and the small aromatic compounds showed a 2% standard deviation in retention factor. In four different monolithic columns, with 10 m*M* sodium borate, pH 8.0, in 80% (v/v) aqueous acetonitrile, the mobilities of formamide were 1.40×10^{-8}, 1.17×10^{-8}, 1.50×10^{-8} and 1.55×10^{-8} m^2/Vs. These results strongly suggest that the in situ sintered and octadecylated monolithic columns can be sufficiently stable and afford reproducible measurements in routine applications.

4. Conclusions

Essentially, there are two methods to prepare

capillary columns with monolithic packing for CEC. In the first method, the capillary is initially filled with a mixture of monomers, porogen and catalyst, then the mixture is polymerized in situ to obtain a highly crosslinked, microporous polymeric monolith. Thereafter, the porogen is removed and the surface of the porous polymer is treated chemically to convert it to a stationary phase having suitable rheogenic and retentive functions. The other method, starts with a conventional capillary column packed with a particulate support. Thereafter, the particles are agglomerated (glued, cemented or sintered) so that the packing becomes a porous monolith. Subsequently, the chromatographic surface may be functionalized in order to impart the desired rheogenic and retentive properties to the column packing.

In the present work, the second approach was taken to prepare silica based reversed-phase monolithic columns by packing fused-silica capillaries with porous silica particles and subsequently sintering them. Finally, in situ octadecylation of the chromatographic surface is carried out in order to impart the desired retentive properties to the column. It was shown that sintering, under controlled conditions, stabilizes column packing and significantly increases the longevity of the column in CEC. It was found that the best results were obtained by packing the column not with raw silica but with octadecylated silica particles which do not bind water strongly. The stability of the monolithic columns was tested by their continuous use over a month in both μ-HPLC and CEC and no untoward changes in the packing structure were observed. The monolithic columns offer separation characteristics comparable to those of the conventional silica packed capillaries, and can be used at atmospheric pressure and in a wide range of organic modifier concentrations in the eluent.

The versatility and stability of the sintered silica monolithic columns are expected to facilitate their employment in CEC at high applied voltages. Monolithic columns are easy to prepare and since they have close resemblance to silica based bonded phases that possess a vast library of applications, they have the potential for routine use. Improvements in the use of these novel columns are aimed at specific applications, such as the separation of carbohydrates and proteins by in situ functionalizing of the stationary bed to obtain the retentive surface most appropriate for the separation.

Acknowledgements

Many thanks to Christian Huber for helpful discussions and suggestions. This work was supported by Grant No. GM 20993 from The National Institutes of Health, US Department of Health and Human Services.

References

[1] N.W. Smith, M.B. Evans, Chromatographia 38 (1994) 649.
[2] V. Pretorius, B.J. Hopkins, J.D. Schieke, J. Chromatogr. 99 (1974) 23.
[3] J.H. Knox, I.H. Grant, Chromatographia 24 (1987) 135.
[4] M.M. Dittmann, G.P. Rozing, J. Chromatogr. A 744 (1996) 63.
[5] W.D. Ross, R.T. Jefferson, J. Chromatogr. Sci. 8 (1970) 386.
[6] T.R. Lynn, D.R. Rushneck, A.R. Cooper, J. Chromatogr. Sci. 12 (1974) 76.
[7] S. Hjertén, J.-L. Liao, R. Zhang, J. Chromatogr. 473 (1989) 273.
[8] J.-L. Liao, R. Zhang, S. Hjertén, J. Chromatogr. 586 (1991) 21.
[9] F. Sveč, J.M.J. Fréchet, Anal. Chem. 64 (1992) 820.
[10] C. Ericson, J.-L. Liao, K. Nakazato, S. Hjertén, J. Chromatogr. A 767 (1997) 33.
[11] E.C. Peters, M. Petro, F. Sveč, J.M.J. Fréchet, Anal. Chem. 69 (1997) 3646.
[12] H. Minakuchi, K. Nakanishi, N. Soga, N. Ishizuka, N. Tanaka, Anal. Chem. 68 (1996) 3498.
[13] S.M. Fields, Anal. Chem. 68 (1996) 2709.
[14] T. Adam, K.K. Unger, M.M. Dittmann, G. Rozing, Presented at the 21st International Symposium on High Performance Liquid Phase Separations and Related Techniques. Birmingham, UK, June 1997, Lecture L-74.
[15] G. Choudhary, Cs. Horváth, J. Chromatogr. A 781 (1997) 161.
[16] C.G. Huber, G. Choudhary, Cs. Horváth, Anal. Chem. 69 (1997) 4429.
[17] R.J. Boughtflower, T. Underwood, C.J. Paterson, Chromatographia 40 (1995) 329.
[18] S.E. van den Bosch, S. Heemstra, J.C. Kraak, H. Poppe, J. Chromatogr. A 755 (1996) 165.
[19] A.J. Moulson, J.M. Herbert, Electroceramics, Chapman and Hall, London, 1992, p. 100.
[20] R.M. German, Ceramics and Glasses, Engineered Materials Handbook, ASM International, 1987, p. 260.
[21] R.M. German, Liquid Phase Sintering, Plenum Press, London, 1985.

[22] R.K. Iler, The Chemistry of Silica, Wiley Interscience, New York, 1976, p. 16.
[23] R.B. Sosman, Ceram. Bull. 43 (1964) 213.
[24] R.B. Sosman, The Phases of Silica, Rutgers University Press, New Brunswick, 1965.
[25] J.W. Jorgenson, K.D. Lukacs, J. Chromatogr. 218 (1981) 209.
[26] J.H. Knox, Chromatographia 26 (1988) 329.
[27] M. von Smoluchowski, Bull. Intern. Acad. Sci. Cracovie 1 (1903) 184.
[28] C. Schwer, E. Kenndler, Anal. Chem. 63 (1991) 1801.
[29] H.G. Barth, F.E. Regnier, J. Chromatogr. 192 (1980) 275.
[30] B. Behnke, E. Bayer, J. Chromatogr. A 680 (1994) 93.
[31] H. Rebscher, U. Pyell, Chromatographia 38 (1994) 737.
[32] C. Yan, D. Schaufelberger, F. Erni, J. Chromatogr. A 670 (1994) 15.
[33] H. Yamamoto, J. Baumann, F. Erni, J. Chromatogr. 593 (1992) 313.
[34] E.sz. Kováts, J. Chromatogr. Libr. 32 (1985) 205.
[35] N.L. Ha, J. Ungvárai, E.sz. Kováts, Anal. Chem. 54 (1982) 2410.
[36] H. Chen, Cs. Horváth, Anal. Methods Instrumentation 1 (1993) 213.
[37] G. Frank, W. Strubert, Chromatographia 6 (1973) 522.
[38] J.A. Rodkey, C.D. Bennett, Biochem. Biophys. Res. Commun. 72 (1976) 1407.
[39] J.D. Peterson, S. Nehrlich, P.E. Oyer, D.F. Steiner, J. Biol. Chem. 250 (1975) 557.
[40] P.W. Moser, E.E. Rickli, J. Chromatogr. 176 (1979) 451.
[41] M. Castagnola, D.V. Rossetti, L. Cassiano, R. Rabino, G. Nocca, B. Giardina, J. Chromatogr. 638 (1993) 327.
[42] K. Otsuka, M. Kashihara, Y. Kawaguchi, R. Koike, T. Hisamitsu, S. Terabe, J. Chromatogr. A 652 (1993) 253.
[43] K. Otsuka, K. Karuhaka, M. Higashimori, S. Terabe, J. Chromatogr. A 680 (1994) 317.
[44] B.L. Karger, L.R. Snyder, Cs. Horváth, An Introduction to Separation Science, Wiley-Interscience, New York, 1973.
[45] Cs. Horváth, H.-J. Lin, J. Chromatogr. 149 (1978) 43.